COWLES FOUNDATION FOR RESEARCH IN ECONOMICS
YALE UNIVERSITY
30 Hillhouse Avenue, New Haven CT 06520 8281

Large Deviations and the Distribution of Price Changes

Laurent Calvet and Adlai Fisher*
Department of Economics, Yale University

Benoit Mandelbrot†
Department of Mathematics, Yale University and
IBM T. J. Watson Research Center

Cowles Foundation Discussion Paper No. 1165

This Draft: September 15, 1997
First Draft: October 1996

*28 Hillhouse Avenue, New Haven, CT 06520-1972. e-mail: lcalvet@minerva.cis.yale.edu, fisher@econ.yale.edu
†10 Hillhouse Avenue, New Haven, CT 06520-8283. e-mail: fractal@watson.ibm.com

COWLES FOUNDATION FOR RESEARCH IN ECONOMICS
YALE UNIVERSITY
30 Hillhouse Avenue, New Haven CT 06520 8281

Abstract

The Multifractal Model of Asset Returns ("MMAR", See Mandelbrot, Fisher, and Calvet, 1997) proposes a class of multifractal processes for the modelling of financial returns. In that paper, multifractal processes are defined by a scaling law for moments of the processes' increments over finite time intervals. In the present paper, we discuss the local behavior of multifractal processes. We employ local Hölder exponents, a fundamental concept in real analysis that describes the local scaling properties of a realized path at any point in time. In contrast with the standard models of continuous time finance, multifractal processes contain a multiplicity of local Hölder exponents within any finite time interval. We characterize the distribution of Hölder exponents by the multifractal spectrum of the process. For a broad class of multifractal processes, this distribution can be obtained by an application of Cramér's Large Deviation Theory. In an alternative interpretation, the multifractal spectrum describes the fractal dimension of the set of points having a given local Hölder exponent. Finally, we show how to obtain processes with varied spectra. This allows the applied researcher to relate an empirical estimate of the multifractal spectrum back to a particular construction of the stochastic process.

Keywords: Multifractal Model of Asset Returns, Multifractal Spectrum, Compound Stochastic Process, Subordinated Stochastic Process, Time Deformation, Scaling Laws, Self-Similarity, Self-Affinity

COWLES FOUNDATION FOR RESEARCH IN ECONOMICS
YALE UNIVERSITY
30 Hillhouse Avenue, New Haven CT 06520 8281

1 Introduction

The Multifractal Model of Asset Returns (MMAR) proposes a class of multifractal processes for the modelling of financial prices. In Mandelbrot, Fisher and Calvet (1997), multifractality is defined by the scaling properties of the processes' moments over different time increments. This "global" definition imposes restrictions on the unconditional distributions of the price process. It pays little attention however to the heterogeneity of price variability across time, which has recently attracted much attention from econometricians.

In this paper, we focus on the "local" behavior of the MMAR. Our approach is based on the local Hölder exponent, a fundamental concept in real analysis that describes the scaling properties of a realized path at any point in time. This concept can be heuristically defined as follows. On a fixed realized path, the infinitesimal variation in price around a date t is of the form:

$$|P(t+dt) - P(t)| \sim C_t (dt)^{\alpha(t)},$$

where $\alpha(t)$ and C_t are respectively called the *local Hölder exponent* and the *prefactor* at t.

In typical financial models, the local Hölder exponent can only take a finite number of values. For instance continuous Itô processes have the property that $\alpha(t) = 1/2$ everywhere. Much recent research on these processes has attempted to model the time-varying volatility, i.e. the prefactor C_t. A good presentation of these advances is contained in Rossi (1997). Financial economists have also used long memory processes based on the Fractional Brownian Motion (FBM) of Mandelbrot and Van Ness (1968). The FBM contains a single local Hölder exponent, its index of self-affinity. Discontinuities or jumps have sometimes been added to these models, and permit local Hölder exponents equal to zero. In short, these traditional financial models contain at most two Hölder exponents along their sample paths.

There is however little justification for this choice, since temporal heterogeneity can be caused by variations in both the local Hölder exponent and the prefactor. We show in this paper that the MMAR captures this possibility and contains a *continuum* of local Hölder exponents. Their distribution can be represented by a renormalized density called the *multifractal spectrum*. In an alternative interpretation, the spectrum describes the fractal dimension of the set of instants having a given local exponent. The statistical self-similarity of these sets accounts for long memory in the process. For a broad class of multifractals, this distribution is obtained by an application of

Cramér's Large Deviation Theory. We derive closed-form expressions for the spectra of particular processes. This allows the applied researcher to relate an empirical estimate of the multifractal spectrum back to a particular construction of the stochastic process.

Section 2 presents a brief review of multifractal measures and processes. Section 3 defines the concept of multifractal spectrum. Section 4 introduces Cramér's Large Deviation Theory and derives the spectrum for a large class of multifractals. Section 5 applies these ideas to the MMAR. Section 6 concludes.

2 Multifractals

This section presents a brief review of multifractal measures and processes. A more detailed discussion of these topics can be found in the companion theoretical paper, Mandelbrot, Fisher and Calvet (1997).

2.1 The Binomial Measure

This section introduces the simplest multifractal, the binomial measure[1] on the compact interval $[0,1]$. This is the limit of an elementary iterative procedure called a *multiplicative cascade*.

Let m_0 and m_1 be two positive numbers adding up to 1. At stage $k=0$, we start the construction with the uniform probability measure μ_0 on $[0,1]$. In the step $k=1$, the measure μ_1 uniformly spreads mass equal to m_0 on the subinterval $[0,1/2]$ and mass equal to m_1 on $[1/2,1]$. Figure 1a represents the density of μ_1 when $m_0=0.6$.

In step $k=2$, the set $[0,1/2]$ is split into two subintervals, $[0,1/4]$ and $[1/4,1/2]$, which respectively receive a fraction m_0 and m_1 of the initial mass $\mu_1[0,1/2]$. We apply the same procedure to the dyadic set $[1/2,1]$ and obtain:

$$\mu_2[0,1/4]=m_0m_0, \qquad \mu_2[1/4,1/2]=m_0m_1,$$
$$\mu_2[1/2,3/4]=m_1m_0, \quad \mu_2[3/4,1]=m_1m_1.$$

An infinite repetition of this scheme generates a sequence of measures (μ_k) that converges to the binomial measure μ. Figure 1b represents the measure μ_4 obtained after $k=4$ steps.

The properties of the binomial are now briefly reviewed. Consider the dyadic interval $[t,t+2^{-k}]$,

[1] The binomial measure is sometimes called the Bernoulli or Besicovitch measure.

where

$$t = 0.\eta_1\eta_2..\eta_k = \sum_{i=1}^{k} \eta_i 2^{-i}$$

in the counting base $b = 2$. Let φ_0 and φ_1 denote the relative frequencies of 0's and 1's in the binary development of t. The measure of the dyadic interval simplifies to:

$$\mu[t, t + 2^{-k}] = m_0^{k\varphi_0} m_1^{k\varphi_1}.$$

The binomial measure has important characteristics common to many multifractals. It is a continuous but singular probability measure. The procedure preserves at each stage the mass of split dyadic intervals and is accordingly called *conservative* or *microcanonical.*

This construction can receive several extensions. For instance at each stage of the cascade, intervals can be split not in 2 but in $b > 2$ intervals of equal size. Subintervals, indexed from left to right by β ($0 \leq \beta \leq b - 1$), receive fractions of the total mass equal to $m_0, .., m_{b-1}$. In order to conserve mass these fractions, also called *multipliers,* are restricted to add up to one: $\sum m_\beta = 1$. This defines the class of *multinomial* measures, which are discussed in Mandelbrot (1989a) and Evertsz and Mandelbrot (1992).

In another extension, the allocation of mass in the cascade becomes random. The multiplier of each subinterval is a discrete random variable M_β that takes values $m_0, m_1, ..., m_{b-1}$ with probabilities $p_0, .., p_{b-1}$. The preservation of mass imposes the additivity constraint: $\sum M_\beta = 1$. Figure 1c shows the random density obtained after $k = 10$ iterations with parameters $b = 2$, $p = p_0 = 0.5$ and $m_0 = 0.6$.

2.2 Multiplicative Measures

Multiplicative measures generalize the previous constructions by allowing multipliers M_β ($0 \leq \beta \leq b - 1$) that are not necessarily discrete, but may be more general random variables. To simplify the presentation, we assume that the multipliers M_β are identically distributed.

We first assume that mass is preserved at every stage of the construction: $\sum M_\beta = 1$. The resulting measure is then called *microcanonical* or *micro-conservative.* Given a date $t = 0.\eta_1...\eta_k$ and a length $\Delta t = b^{-k}$, the measure $\mu(\Delta t)$ of the b-adic cell $[t, t + \Delta t]$ satisfies:

$$\mu(\Delta t) = M(\eta_1)M(\eta_1, \eta_2)...M(\eta_1, ..., \eta_k).$$

Since multipliers at different stages of the cascade are independent, the moments of the measure are of the form: $\mathbb{E}\left[\mu(\Delta t)^q\right] = \left[\mathbb{E}(M^q)\right]^k$ for all admissible $q \geq 0$. With the notation $\tau(q) = -\log_b \mathbb{E}(M^q) - 1$, this expression can be rewritten:

$$\mathbb{E}\left[\mu(\Delta t)^q\right] = (\Delta t)^{\tau(q)+1}.$$

The measure thus satisfies the scaling property characterizing multifractals.[2]

Modifying the previous construction, we now choose that the multipliers M_β be statistically independent. Each iteration only conserves mass "on average" in the sense that $\mathbb{E}(\sum M_\beta) = 1$ or $\mathbb{E}M = 1/b$. The corresponding measure is then called *canonical* or *canonical.* Its total mass, denoted Ω, is generally random[3], and the mass of a b-adic cell takes the form:

$$\mu(\Delta t) = \Omega(\eta_1, ..., \eta_k) M(\eta_1) M(\eta_1, \eta_2) ... M(\eta_1, ..., \eta_k).$$

We note that $\Omega(\eta_1, ..., \eta_k)$ has the same distribution as Ω. The measure thus satisfies the scaling relationship:

$$\mathbb{E}\left[\mu(\Delta t)^q\right] = \mathbb{E}(\Omega^q)\,(\Delta t)^{\tau(q)+1},$$

which characterizes multifractals.

2.3 Multifractal Processes

The concept of multifractality easily extends to stochastic processes.

Definition 1 *A stochastic process $\{X(t)\}$ is called multifractal if it satisfies:*

$$\mathbb{E}\left(|X(t)|^q\right) = c(q) t^{\tau(q)+1}, \text{ for all } t \in \mathcal{T},\ q \in \mathcal{Q}, \tag{1}$$

where $\mathcal{T}$ and $\mathcal{Q}$ are intervals on the real line, and $\tau(q)$ and $c(q)$ are functions with domain $\mathcal{Q}$. Moreover, we assume that $\mathcal{T}$ and $\mathcal{Q}$ have positive lengths, and that $0 \in \mathcal{T}$, $[0,1] \subseteq \mathcal{Q}$.

The function $\tau(q)$ is called the *scaling function* of the multifractal process. It is concave and has intercept $\tau(0) = -1$. Multifractals are called *uniscaling* when $\tau(q)$ is linear, and *multiscaling* otherwise. We now justify this terminology and show in which sense multiscaling processes have a multiplicity of local scales.

[2] To simplify exposition, we directly define multifractals via this property. For a more rigorous treatment, which begins by defining multifractals as statistically self-similar measures, and develops their properties, see Mandelbrot (1989a).

[3] The random variable Ω has interesting distributional and tail properties that are discussed in Mandelbrot (1989a).

3 Local Hölder Exponents and the Multifractal Spectrum

3.1 Local Hölder Exponent

We first introduce a concept borrowed from real analysis which characterizes the smoothness of a function at a given date.

Definition 2 *Let g be a function defined on the neighborhood of a given date t. The number*

$$\alpha(t) = Sup\ \{\beta \geq 0 : |g(t + \triangle t) - g(t)| = O(|\triangle t|^{\beta})\ \ as\ \triangle t \to 0\}$$

is called the Hölder exponent of g at t.

The Hölder exponent is sometimes called the "local strength of singularity." It always exists and is generally valued in $[-\infty, +\infty]$. We note that $\alpha(t)$ is non-negative if (and only if) the function g is bounded around t. For simplicity, this paper only considers functions locally bounded on their domains, which guarantees the non-negativity of all Hölder exponents.

Definition 3.1 readily extends to measures defined on the real line. At a given date t, the local exponent of a measure is simply defined as the local exponent of its c.d.f. Since measures are bounded, the Hölder exponents are everywhere non-negative.

The Hölder exponent receives an intuitive interpretation when the infinitesimal variations of the function satisfy the scaling relationship[4]:

$$|g(t + \triangle t) - g(t)| \sim C_t(\triangle t)^{\alpha(t)}, \tag{2}$$

where the positive constant C_t is called *prefactor*. The local Hölder exponent then appears as a *local scale* in the sense of fractal geometry. This approach to Hölder exponents is further discussed in Mandelbrot (1982, pp. 373-374).

From equation (2), we can easily compute the exponents of several examples. For instance the local scale is 0 at points of discontinuity, and 1 at differentiable points where $g' \neq 0$. The Hölder exponents of elementary functions are thus integers almost everywhere (a.e.). Non integer exponents appear with greater frequency in very winding continuous functions. For instance the jagged paths of Brownian motions are characterized by Hölder exponents equal to 1/2. This property holds in fact for all continuous Itô processes. Fractional Brownian Motions $B_H(t)$ also have a unique Hölder exponent, their index of self-affinity H. By contrast, the next section shows that multifractals contain a multiplicity of local scales.

[4]The expression $(\Delta t)^{\alpha(t)}$ is an example of "non-standard infinitesimal", as developed by Abraham Robinson.

3.2 The Multifractal Spectrum

Remark 1 *Multifractality, like Hölder exponent, is a concept that can be applied equally well to functions and measures, deterministic or stochastic, with some minor adjustments. The remainder of the paper discusses multifractal measures and processes simultaneously. We hope this approach to presentation will provide the greatest exposure to mathematical formulations of multifractality without being unnecessarily confusing.*

The continuous time stochastic processes commonly used to model financial prices can each be characterized by a unique Hölder exponent. (See the examples at the end of the previous section.) In Mandelbrot, Fisher and Calvet (1997), we presented an alternative model which can be distinguished by the presence of a continuum of Hölder exponents.

The literature on multifractals has developed a convenient representation for the distribution of Hölder exponents within a measure. This representation is typically called the multifractal spectrum, and is denoted by the function $f(\alpha)$, which we now describe.

It is easy to show from definition 3.1 that the Hölder exponent of a continuous path $g(t)$ at a date t is the limsup of the ratio

$$\ln L(t, \triangle t)/\ln(\triangle t) \text{ as } \triangle t \to 0,$$

where for convenience we define $L(t, \triangle t) \equiv |g(t + \triangle t) - g(t)|$. This suggests a method for estimating the probability that a point randomly chosen on the interval $[0, T]$ will have a given Hölder exponent. We iteratively subdivide the interval into b^k equal sized pieces, k denoting the stage in the sequence of subdivisions. At each stage, we calculate the finite quantities $L(t_i, b^{-k}T)$ for each of the b^k subdivisions. Define the coarse Hölder exponent:

$$\alpha_k(t_i) \equiv \ln L(t_i, b^{-k}T)/\ln(b^{-k}).$$

Partition the range of α's into small non-overlapping intervals, $(\overline{\alpha}_j, \overline{\alpha}_j + \triangle\alpha]$, and denote by $N_k(\overline{\alpha}_j)$ the number of coarse Hölder exponents $\alpha_k(t_i)$ contained in each interval $(\overline{\alpha}_j, \overline{\alpha}_j + \triangle\alpha]$. In the limit, as $k \to \infty$, the ratio $N_k(\alpha)/b^k$ converges to the probability that a randomly selected point t has Hölder exponent α.[5]

While this intuitive method of representing the distribution of different Hölder exponents within a path is absolutely correct, and can be made rigorous via the law of large numbers, it will fail to

[5]Note that this probability is the same as the Lebesgue measure of the set of points having Holder exponent α, divided by T.

distinguish between multifractal processes and unifractal processes.

Multifractals typically have the property that a single Hölder exponent α_0 predominates, in the sense that the set of instants with exponent α_0 carries all of the Lebesgue measure. Nonetheless, the other Hölder exponents matter even more. In fact, most of the mass of a multifractal measure, or most of the variation of a multifractal function, concentrates on a set of instants with Hölder exponent different from α_0.

It should come as no surprise, given the example of the Poisson process and other *discontinuous* processes, that events that occur on sets of Lebesgue measure zero can be extremely important components of the total variation of a stochastic process. It may be something more of a surprise to find that, for a *continuous* stochastic process, events occurring on a set of Lebesgue measure zero can contribute almost all of the variation. Such is the case with multifractals.

Mandelbrot (1989a), applying Cramér's large-deviation theory, shows that the renormalization required to discriminate between multifractality and unifractality is obtained via logarithmic transforms of both numerator and denominator in the standard frequency representation of probability theory.

Definition 3 *Assume a (possibly random) function $g(t)$. Using the same iterative procedure and notation as above, let*

$$f(\alpha) \equiv \lim \left\{ \frac{\ln N_k(\alpha)}{\ln b^k} \right\} \;\; \text{as } k \to \infty. \tag{3}$$

If $f(\alpha)$ is defined (i.e. the limit exists) and positive on a support larger than a single point, then we say that $g(t)$ is a multifractal.

The above definition, which applies to functions or random processes, directly extends to measures and random measures by consideration of the c.d.f.

3.3 Interpretation of $f(\alpha)$ as the Fractal Dimension of the Set of Points with Local Hölder Exponent α

For the class of multifractals discussed in this paper, Frisch and Parisi (1985), and Halsey et al. (1986) interpreted $f(\alpha)$ as the fractal dimension of the set of points having local Hölder exponent α. For the reader not familiar with fractal geometry, we first introduce the concept of Hausdorff-Besicovitch (or fractal) dimension.

Fractal geometry considers irregular and winding structures, such as coastlines and snowflakes, which are not well described by their Euclidean length. For instance, a geographer measuring the length of a coastline will find very different results as she increases the precision of her measurement. In fact, the structure of the coastline is usually so intricate that the measured length diverges to infinity as the geographer's measurement scale goes to zero. For this reason, we cannot use the Euclidean length to compare two different coastlines.

In this situation, it is natural to introduce a new concept of dimension. Given a precision level $\varepsilon > 0$, we consider coverings of the coastline with balls of diameter ε. Let $N(\varepsilon)$ denote the smallest number of balls required for such a covering. The approximate length of the coastline is defined by:

$$L(\varepsilon) = \varepsilon N(\varepsilon).$$

In many cases, $N(\varepsilon)$ satisfies a power law as ε goes to zero:

$$N(\varepsilon) \sim \varepsilon^{-D},$$

where D is a constant called the *fractal or Hausdorff-Besicovitch dimension.*

As the precision ε goes to zero, the number of balls $N(\varepsilon)$ grows more quickly for more winding coastlines. The fractal or Hausdorff-Besicovitch dimension can thus be used to discriminate, or "measure", the complexity of coastlines.

The fractal dimension can be defined for any bounded subset of a Euclidean space. It has sound mathematical foundations due to Felix Hausdorff (1919). An outline of this construction is presented in Appendix 7.1. There are many discussions of this topic in the literature, including the expositions of Billingsley (1967), Rogers (1970) and Mandelbrot (1982).

Hausdorff-Besicovitch dimension helps to analyze the structure of a fixed multifractal. For any $\alpha \geq 0$, we can define the set $T(\alpha)$ of instants with Hölder exponent α. As any subset of the real line, $T(\alpha)$ has a fractal dimension $D(\alpha)$, which satisfies $0 \leq D(\alpha) \leq 1$. It can be shown that for a large class of multifractals, the dimension $D(\alpha)$ coincides with the multifractal spectrum $f(\alpha)$.

In the case of measures, we can provide a heuristic interpretation of this result based on coarse Hölder exponents. Denoting by $N(\alpha, \Delta t)$ the number of intervals $[t, t + \Delta t]$ required to cover $T(\alpha)$, we infer from Equation (3) that: $N(\alpha, \Delta t) \sim (\Delta t)^{-f(\alpha)}$. Using a partition of $[0, T]$ in intervals of length Δt, we rewrite the total mass

$$\mu[0,T] = \sum \mu(\Delta t) \sim \sum (\Delta t)^{\alpha(t)} ,$$

and rearrange it as a sum over Hölder exponents:

$$\mu[0,T] \sim \int (\Delta t)^{\alpha - f(\alpha)} \, d\alpha.$$

The integral to the right-hand side is dominated by the contribution of the Hölder exponent α_1 that minimizes $\alpha - f(\alpha)$. The total measure can then be expressed as:

$$\mu[0,T] \sim (\Delta t)^{\alpha_1 - f(\alpha_1)}$$

Since the total mass $\mu[0,T]$ is positive, we infer that $f(\alpha_1) = \alpha_1$, and $f(\alpha) \leq \alpha$ for all α. When f is differentiable, the coefficient α_1 also satisfies $f'(\alpha_1) = 1$. The spectrum $f(\alpha)$ then lies under the 45^o line, with tangential contact at $\alpha = \alpha_1$.

We finally note that this heuristic discussion has an interesting graphical interpretation. For various levels of the Hölder exponent α, Figure 1d represents the "cut" consisting of the subintervals with coarse exponents lower than α. We see that when the number of iterations k is sufficiently large, these cuts display a self-similar structure.

4 Large Deviation Theory and Multiplicative Cascades

This section examines the local properties of multiplicative measures. Their multifractal spectrum $f(\alpha)$ is derived from a result of probability theory that is becoming well-known, Cramér's Large Deviation theorem. Closed form expressions for $f(\alpha)$ are then provided in some examples. These results have important consequences for financial prices. In the Multifractal Model of Asset Returns (MMAR), prices follow a compound process $B_H[\theta(t)]$, where $B_H(t)$ is a fractional Brownian motion, and trading time $\theta(t)$ is the c.d.f. of a random self-similar measure μ. Section 5 will show that the price process directly inherits its multifractality from the measure. In particular, the spectra of the price process and the measure are directly related by: $f_p(\alpha) \equiv f_\mu(\alpha/H)$. The present section thus provides essential information on a large class of multifractal price processes.

4.1 The Statistical Properties of the Coarse Hölder Exponent

We consider a measure μ defined as the limit of a multiplicative cascade. To simplify the presentation, μ is first assumed to be micro-conservative, while section 4.1.4. will discuss the case of canonical measures.

After k iterations of the construction procedure, we know the measures:

$$\mu[t, t+\Delta t] = M(\eta_1)...M(\eta_1, .., \eta_k), \tag{4}$$

of b^k intervals of the form $[t, t+\Delta t]$, where $\Delta t = b^{-k}$ and $t = 0.\eta_1..\eta_k = \sum_{i=1}^{k} \eta_i b^{-i}$ is a b-adic number. This corresponds to the knowledge of the empirical researcher, whose data consist of the observation of finite variations. Alternatively, the researcher can consider the coarse Hölder exponents:

$$\begin{aligned} \alpha_k(t) &= \frac{\ln \mu[t, t+\Delta t]}{\ln \Delta t} \\ &= -\frac{1}{k}\left[\log_b M(\eta_1) + ... + \log_b M(\eta_1, .., \eta_k)\right]. \end{aligned} \tag{5}$$

In empirical work, we would like to view the b^k coarse Hölder exponents as draws of a random variable α_k. This can be done in two different cases, as is now shown.

For *deterministic* measures μ (such as the binomial), we consider the mass of a *random* cell. More specifically, we randomly draw integers $\eta_1..\eta_k$, and thus the b-adic number $t = 0.\eta_1..\eta_k$. We denote α_k the coarse exponent of the random cell. The observed exponents $\alpha_k(t)$ can then be viewed as particular draws of the random variable α_k.

When the measure μ is *randomly* generated, we choose a *fixed* cell $[t, t+\Delta t]$. The measure $\mu[t, t+\Delta t]$ is random because of the multipliers $M(\eta_1)$,..., $M(\eta_1, .., \eta_k)$. In this case, all cells are essentially the same. The coarse exponents $\alpha_k(t)$ are identically distributed across b-adic cells, and can again be viewed as draws of a random variable α_k. In particular, randomizing the cell $[t, t+\Delta t]$ does not alter the distribution of α_k.

In this section, we use the random variable α_k to study the multifractal spectrum $f(\alpha)$ of the measure μ. The loose intuition is the following. The multifractal spectrum is obtained by forming histograms of the coarse Hölder exponents. It is sometimes reasonable to replace this construction by independent draws of the random variable α_k. The spectrum $f(\alpha)$ can then be directly derived from the asymptotic distribution of α_k.

By equation (5), the Hölder exponent α_k is the sample sum of k iid random variables. Denoting by V_i the addend $-\log_b M(\eta_1, .., \eta_i)$, we rewrite α_k as the average of iid random variables:

$$\alpha_k = \frac{1}{k} \sum_{i=1}^{k} V_i. \tag{6}$$

For large values of k, the distribution of α_k can be analyzed with the main tools of probability theory: the Strong Law of Large Numbers (SLLN), the Central Limit Theorem (CLT) and Large Deviation Theory (LDT). While SLLN implies convergence to a most probable exponent, CLT and LDT respectively provide information on the bell and the tail of α_k.

4.1.1 Law of Large Numbers and Most Probable Hölder Exponent α_0

By the SLLN, the random variable α_k converges almost surely to

$$\alpha_0 = \mathbb{E}\, V_1 = -\mathbb{E}\, \log_b M. \tag{7}$$

Since $\mathbb{E}\, M = 1/b$, Jensen's inequality implies that $\alpha_0 > 1$. As $k \to \infty$, we expect that almost all coarse Hölder exponents are contained in a small neighborhood of α_0. The standard histogram $N_k(\alpha)/b^k$ thus collapses for large values of k, as in the informal discussion of Section 3.2.

The other coarse Hölder exponents do matter however. In fact, most of the mass concentrates on intervals with Hölder exponents that are bounded away from α_0, as is now shown. Let T_k denote the set of b-adic cells with a Hölder exponent greater than $(1 + \alpha_0)/2$. For large values of k, we expect that "almost all" cells belong to T_k. However their mass:

$$\sum_{t \in T_k} \mu[t, t + \Delta t] = \sum_{t \in T_k} (\Delta t)^{\alpha_k(t)} \le b^k (\Delta t)^{(\alpha_0+1)/2} = b^{-k(\alpha_0-1)/2}$$

vanishes as k goes to infinity. The mass thus concentrates on these few b-adic intervals which do not belong to T_k. Information on these "rare events" is presumably contained in the tail of the random variable α_k.

4.1.2 Central Limit Theorem and the Shape of $f(\alpha)$ around α_0

Assuming that V_1 has finite variance σ^2, we can apply the CLT:

$$\sqrt{k}(\alpha_k - \alpha_0) \xrightarrow{d} N(0, \sigma^2),$$

which can be rewritten in terms of histogram:

$$\frac{N_k}{N} \sim \frac{1}{\sqrt{2\pi\sigma^2/k}} \exp\left[-\frac{1}{2}\left(\frac{\alpha-\alpha_0}{\sigma/\sqrt{k}}\right)^2\right].$$

By taking logarithms, we get:

$$f(\alpha) \sim 1 - \frac{1}{2\ln b}\left(\frac{\alpha-\alpha_0}{\sigma}\right)^2.$$

The CLT thus shows that the multifractal spectrum is locally quadratic around the most probable exponent α_0.

4.1.3 Multifractal Spectrum and Large Deviation Theory

We now return to the construction of the multifractal spectrum $f(\alpha)$. As in Section 3.2, we subdivide the interval $[0,T]$ into b^k intervals of size $\Delta_k t = b^{-k}T$. Similarly, we partition the range of α's into intervals of length $\Delta\alpha$, and denote $N_k(\overline{\alpha}_j)$ the number of coarse Hölder exponents in the interval $(\overline{\alpha}_j, \overline{\alpha}_j + \Delta\alpha]$.

For large values of k, we write the heuristic relation:

$$\frac{1}{k}\log_b\left[\frac{N_k(\overline{\alpha}_j)}{b^k}\right] \sim \frac{1}{k}\log_b \mathbb{P}\left\{\overline{\alpha}_j < \alpha_k \leq \overline{\alpha}_j + \Delta\alpha\right\}, \tag{8}$$

For multinomial measures, this relation holds exactly for any k because the coarse Hölder exponent is discrete. In more general cases, this heuristic relation is postulated. We now want to study the left-hand side of (8). We see that it hinges on the asymptotic tail properties of the coarse Hölder exponent α_k.

The tail properties of random variables are the object of Large Deviation Theory. In 1938, H. Cramér established the following important theorem under conditions that were gradually weakened.

Theorem 4 *Let $\{X_k\}$ denote a sequence of iid random variables. Then as $k \to \infty$,*

$$\frac{1}{k}\ln\mathbb{P}\left\{\frac{1}{k}\sum_{i=1}^{k} X_i > \alpha\right\} \to \underset{q}{Inf}\ln\left[\mathbb{E}\, e^{q(\alpha - X_1)}\right],$$

for any $\alpha > \mathbb{E}X_1$.

There are many proofs of this theorem in the literature, including Durrett (1991). More general references on Large Deviation Theory can be found in Deutschel and Stroock (1989).

We now apply Cramér's theorem to the random variable α_k:

$$\frac{1}{k}\log_b \mathbb{P}\left\{\alpha < \alpha_k\right\} \to \delta(\alpha) \equiv \operatorname*{Inf}_q \log_b \left[\mathbb{E}\, e^{q(\alpha - V_1)\ln b}\right] \qquad \text{as } k \to \infty,$$

for any $\alpha > \alpha_0$. Similarly when $\alpha < \alpha_0$, it is easy to show that: $k^{-1}\log_b \mathbb{P}\left\{\alpha_k < \alpha\right\}$ converges to $\delta(\alpha) \equiv \operatorname{Inf}\log_b \left[\mathbb{E}\, e^{q(\alpha - V_1)\ln b}\right]$.

Since $V_1 = -log_b M$, the limit $\delta(\alpha)$ can be rewritten:

$$\delta(\alpha) = \operatorname*{Inf}_q \left[\log_b(\mathbb{E}\, b^{\alpha q + q \log_b M})\right] = \operatorname*{Inf}_q \left[\alpha q + \log_b(\mathbb{E}\, M^q)\right] \tag{9}$$

for all values of α. Consistently with the notations of Section 2.2, it is convenient to define the scaling function:

$$\tau(q) \equiv -\log_b(\mathbb{E}\, M^q) - 1. \tag{10}$$

We obtain: $\delta(\alpha) = \operatorname*{Inf}_q [\alpha q - \tau(q)] - 1$, which shows that $\delta(\alpha) + 1$ is the Legendre transform of $\tau(q)$.

Returning to the histogram construction, we see that:

$$\frac{1}{k}\log_b \mathbb{P}\left\{\overline{\alpha}_j < \alpha_k\right\} \to \delta(\overline{\alpha}_j) \text{ for any } \overline{\alpha}_j > \alpha_0.$$

In fact, it is easy to show (see Appendix 7.2) that

$$\mathbb{P}\left\{\overline{\alpha}_j < \alpha_k \leq \overline{\alpha}_j + \Delta\alpha\right\} \sim \mathbb{P}\left\{\overline{\alpha}_j < \alpha_k\right\}. \tag{11}$$

A similar reasoning holds when $\overline{\alpha}_j < \alpha_0$. Therefore the right-hand side of (8) converges to $\delta(\overline{\alpha}_j)$, which establishes the following proposition.

Proposition 5 *The multifractal spectrum $f(\alpha)$ is the Legendre transform:*

$$f(\alpha) = \mathop{Inf}_q [\alpha q - \tau(q)]$$

of the scaling function $\tau(q)$.

This proposition lays the foundations of our empirical work. The companion empirical paper, Fisher, Calvet and Mandelbrot (1997) develops a simple estimation procedure for the scaling function $\tau(q)$. A Legendre transform then yields an estimate of the multifractal spectrum $f(\alpha)$.

The previous discussion showed that $f(\alpha)$ is the limit of:

$$\begin{aligned} k^{-1}\log_b \mathbb{P}\{\alpha_k > \alpha\} + 1 \qquad &\text{if } \alpha > \alpha_0, \\ k^{-1}\log_b \mathbb{P}\{\alpha_k < \alpha\} + 1 \qquad &\text{if } \alpha < \alpha_0, \end{aligned}$$

which gives additional information on the spectrum. We note in particular that $f(\alpha) \leq 1$, $f(\alpha)$ increases for $\alpha < \alpha_0$ and decreases for $\alpha > \alpha_0$; the multifractal spectrum is thus hump-shaped. It is easy to show that $\alpha_0 q - \tau(q)$ is minimal when $q = 0$, and thus $f(\alpha_0) = -\tau(0) = 1$. This result receive a simple interpretation in terms of fractal dimension: the set of instants with exponent α_0 has a Lebesgue measure equal to one.

We have thus established that the spectrum can be obtained from LDT. This result is sometimes viewed as the correct definition of $f(\alpha)$. There is no unique definition of the multifractal spectrum in the literature, which represents a frequent source of confusion. In this paper, we have successively viewed the spectrum $f(\alpha)$ as:

(D1) the limit of a renormalized histogram of coarse Hölder exponents,

(D2) the fractal dimension of the set of instants with Hölder exponent α,

(D3) the limit of $k^{-1}\log_b \mathbb{P}\{\alpha_k > \alpha\} + 1$ provided by Large Deviation Theory.

These definitions do not always coincide. For instance (D1) and (D2) imply that $f(\alpha)$ is non-negative, while (D3) imposes no such restriction. The three definitions do agree however for some measures, such as the (deterministic or random) multinomials. Peyrière (1991) shows more generally that definitions (D1) and (D2) coincide for a large class of multifractals.

When it occurs, the conflict between these definitions should not be viewed as a troubling paradox. After all, we could simply choose one of the above properties as the correct definition of the spectrum. It turns out however that the most appropriate definition depends on the particular situation studied. Recent research also shows that "conflict" between the various spectra contains much information on the underlying multifractal. We now present an example of what can be learned from these discrepancies.

Consider the possibility that $f(\alpha)$ can take negative values for some α's according to definition (D3). It can be shown that these α's are rare coarse exponents, which can only be observed in few random measures. Such α's, which are only revealed by examining a large number of measures, are called *latent.* They contrast with *manifest* α's for which $f(\alpha) > 0$. Latent values have the additional property to control the high and low moments of the measure. The spectrum given by LDT thus contains information on the variability of sample histograms, which illustrates the complementarity of these two definitions. Mandelbrot (1989b) provides further discussion of this topic.

4.1.4 Extension to Canonical Cascades

We now generalize the previous results to canonical measures. With the notations of section 2.2, the coarse Hölder exponent $\alpha_k(t) = \ln \mu[t, t + \Delta t]/\ln \Delta t$ satisfies:

$$\alpha_k(t) = -\frac{1}{k} \log_b \Omega(\eta_1, ..., \eta_k) - \frac{1}{k} \left[\log_b M(\eta_1) + ... + \log_b M(\eta_1, .., \eta_k)\right]. \tag{12}$$

It is the sum of a "high frequency" component, $-\log_b \Omega(\eta_1, ..., \eta_k)/k$, and of the familiar "low frequency" average:

$$\alpha_{k,L}(t) = -\frac{1}{k} \left[\log_b M(\eta_1) + ... + \log_b M(\eta_1, .., \eta_k)\right].$$

We expect $\alpha_{k,L}(t)$ to dominate the asymptotic behavior of the coarse Hölder exponent.

By the SLLN, $\alpha_k(t)$ converges almost surely to $\alpha_0 = -E \log_b M$. We can then apply Large Deviation Theory to $\alpha_{k,L}(t)$, and view $f(\alpha)$ as the limit of:

$$\begin{aligned} &k^{-1} \log_b \mathbb{P}\left\{\alpha_{k,L}(t) > \alpha\right\} + 1 \qquad \text{if } \alpha > \alpha_0, \\ &k^{-1} \log_b \mathbb{P}\left\{\alpha_{k,L}(t) < \alpha\right\} + 1 \qquad \text{if } \alpha < \alpha_0. \end{aligned}$$

CLT then applies as in section 4.1.3.

Canonical measures allow that $M > 1$ with positive probability. It is then possible to obtain $\alpha_{k,L}(t) < 0$, and to define the multifractal spectrum for negative α's. These negative values, called *virtual*, cannot correspond to Hölder exponents since the measure is bounded. They describe the "low-frequency" component of the coarse exponent and thus provide important information on the generating mechanism. This topic is further discussed in Mandelbrot (1989b, 1990), and remains an active research area in mathematics.

4.2 Examples

The new characterization of the multifractal spectrum given in (D3) is now used to derive explicit formulae for $f(\alpha)$. These results are important for empirical work. They allow identification of a multiplicative cascade from its multifractal spectrum. This method is implemented in the companion empirical paper.

4.2.1 Multinomial Measures

We first examine the multinomial measures, which are either deterministic or random. Consistently with the notations of Section 2.1, a b-adic interval $[t, t+b^{-k}]$ has measure: $\mu[t, t+b^{-k}] = m_0^{k\varphi_0} m_1^{k\varphi_1} ... m_{b-1}^{k\varphi_{b-1}}$, and coarse Hölder exponent:

$$\alpha_k(t) = -\sum_{i=0}^{b-1} \varphi_i \log_b m_i.$$

We note in particular that coarse Hölder exponents are bounded, with lower bound $\alpha_{\min} = \min(-\log_b m_i)$ and upper bound $\alpha_{\max} = \max(-\log_b m_i)$. We also know from (7) that

$$\alpha_0 = -\frac{1}{b}\sum_{i=0}^{b-1} \log_b m_i$$

is the most probable exponent.

We now turn to the multifractal spectrum. From (10), the scaling function $\tau(q)$ satisfies:

$$\tau(q) = -\log_b \left(\sum_{i=0}^{b-1} m_i^q \right)$$

for all q on the real line. We note that $\tau(q)$ is a strictly concave and increasing function. It is also asymptotically linear for unbounded values of q :

$$\begin{aligned} \tau(q) &\sim q\alpha_{\max} \qquad \text{as } q \to -\infty, \\ \tau(q) &\sim q\alpha_{\min} \qquad \text{as } q \to +\infty. \end{aligned}$$

It is easy to show that the exponents $\alpha_{\min}$, α_0 and $\alpha_{\max}$ respectively correspond to $q = +\infty$, 0, $-\infty$. This implies that the spectrum is hump-shaped and reaches its maximum at α_0. We know moreover that $f(\alpha) = 0$ and $|f'(\alpha)| = +\infty$ for $\alpha = \alpha_{\min}$, $\alpha_{\max}$. The multifractal spectrum is in particular non-negative on its domain.

In the case of the binomial ($b = 2$), an explicit formula is available for $f(\alpha)$:

$$\begin{aligned} f(\alpha) &= -\frac{\alpha_{\max} - \alpha}{\alpha_{\max} - \alpha_{\min}} \log_2 \left(\frac{\alpha_{\max} - \alpha}{\alpha_{\max} - \alpha_{\min}} \right) \\ &\quad - \frac{\alpha - \alpha_{\min}}{\alpha_{\max} - \alpha_{\min}} \log_2 \left(\frac{\alpha - \alpha_{\min}}{\alpha_{\max} - \alpha_{\min}} \right). \end{aligned} \tag{13}$$

Appendix 7.3 presents a derivation of this result. A graphical representation of $f(\alpha)$ is given in Figure 2a.

We finally note that definitions $(D1) - (D3)$ of the spectrum coincide for these measures. Appendix 7.3. shows that definitions $(D1)$ and $(D3)$ coincide. Billingsley (1967) establishes that $(D2)$ also leads to (13).

4.2.2 A Discrete Multiplicative Cascade

We consider a multiplicative measure in which the random variables V_k have Poisson distributions $p(x) = e^{-\gamma}\gamma^x/x!$. By (7), the most probable exponent is $\alpha_0 = \gamma$. The sum $V_1 + ... + V_k$ is also Poisson, with probabilities $p_k(x) = e^{-k\gamma}(k\gamma)^x/x!$. This allows to prove (see Appendix 7.4) that:

$$f(\alpha) = 1 - \frac{\gamma}{\ln b} + \alpha \log_b(\gamma e/\alpha).$$

We note that the multifractal spectrum is defined on the unbounded set $[0, +\infty)$. It is hump-shaped and reaches its maximum at $\alpha_0 = \gamma$. The spectrum takes values: $f(\alpha_0) = 1$, $f(+\infty) = -\infty$. We observe in particular that $f(\alpha)$ is negative for large values of α, i.e. there exist latent α's. There also small latent values when $f(0) = 1 - \gamma/\ln b$ is negative. A graphical representation of the spectrum is provided in Figure 2b.

4.2.3 Continuous Multipliers

We now assume that the multiplier has a continuous density. We denote $p(\alpha)$ the density of $-\log_b M$, and $p_k(\alpha)$ the density of the k-th convolution product of p. We infer from equation (6) that the coarse grain Hölder exponent α_k has density $kp_k(k\alpha)$. In this case, we can apply the following version of Cramér's theorem.

Theorem 6 *The spectrum of a multiplicative measure satisfies*

$$f(\alpha) = 1 + \lim_{k \to \infty} \frac{1}{k} \log_b[kp_k(k\alpha)]$$

whenever the multipliers have a continuous density $p(\alpha)$.

We apply this theorem to several examples.

A- The Gamma Distribution

Consider a multiplicative measure generated by a Gamma density:

$$p(x) = \beta^{\gamma} x^{\gamma-1} e^{-\beta x}/\Gamma(\gamma),$$

with parameters β, $\gamma > 0$. By section (7), the most probable Hölder exponent is $\alpha_0 = \gamma/\beta$.

The sum of two Gamma random variables of respective parameters (β, γ) and (β, γ') has a Gamma distribution with parameter $(\beta, \gamma + \gamma')$. Therefore $p_k(x) = \beta^{k\gamma} x^{k\gamma-1} e^{-\beta x}/\Gamma(k\gamma)$. Using Stirling's approximation, it is then easy to show that $\frac{1}{k} \ln[kp_k(k\alpha)]$ converges to $\gamma \ln(\alpha\beta/\gamma) - \alpha\beta + \gamma$, and thus

$$f(\alpha) = 1 + \gamma \log_b(\alpha\beta/\gamma) + (\gamma - \alpha\beta)/\ln b.$$

f is defined on $(0, \infty)$. It is hump-shaped and reaches its maximum at $\alpha = \alpha_0$. We note that $f(\alpha_0) = 1$ and $f(\alpha) \to -\infty$ when α goes either to 0 or $+\infty$. There are thus small and large latent α's. A graphical representation of the spectrum is provided in Figure 2c.

It is in fact quite simple to construct a multiplicative cascade for which $V = -log_b M$ has density $p(x)$. Consider the procedure of Section 2.2 with $b = 2$. Assume that at any stage k, the multipliers $M(\eta_1, ..., \eta_{k-1}, 0)$ and $M(\eta_1, ..., \eta_{k-1}, 1)$ are uniformly distributed over $[0, 1]$ and add up to unity. For any $m \in [0, 1]$, we know that $\mathbb{P}\{M(\eta_1, ..., \eta_k) < m\} = m$. Since by definition $V_k = -\log_2 M(\eta_1, ..., \eta_k)$, we infer that $\mathbb{P}\{V_k > x\} = 2^{-x}$, and V_k has a Gamma distribution with parameters $\beta = \ln 2$, $\gamma = 1$.

B- The Gaussian Distribution

We now assume that V_k has a Gaussian density:

$$p(x) = (2\pi\sigma^2)^{-1/2} \exp[-(x - \lambda)^2/2\sigma^2].$$

The random multiplier M is log-normal, which implies that $M > 1$ with positive probability. Therefore the conservation of mass cannot hold locally and the multiplicative measure is not microcanonical.

The computation of the multifractal spectrum is however very straightforward. We easily see that: $\frac{1}{k}\ln[kp_k(k\alpha)]$ converges to $-(\alpha-\lambda)^2/2\sigma^2$, and thus

$$f(\alpha) = 1 - \frac{1}{2\ln b}\left(\frac{\alpha-\lambda}{\sigma}\right)^2.$$

The multifractal spectrum is quadratic and defined on the real line. f is hump-shaped and symmetric around its maximum at $\alpha_0 = \lambda$. We note moreover that $f(\lambda) = 1$, and $f(\alpha) \to -\infty$ when $|\alpha| \to \infty$. The multifractal spectrum is graphically represented in Figure 2*d*.

Since f takes negative values, the multiplicative measure contains latent α's, as some of the previous examples. It is also the first case in which the multifractal spectrum is defined for negative values of α. As discussed in Section 4.1.2, these virtual α's appear because the generating mechanism is not micro-conservative and creates mass in some stages of the construction.

C- The Cauchy Distribution

We now assume that $V_k = -\log_b M$ has a Cauchy density: $p(x) = 1/[\pi(1+x^2)]$. Since the multiplier $M = b^{-V}$ has infinite moments of all orders, the multiplicative measure is not even canonical. We can examine by curiosity how the multifractal formalism applies in this case. By Lévy stability, $\alpha_k = \sum V_i/k$ has the same distribution as V_1. Consequently, $\frac{1}{k}\log_b \mathbb{P}\{\alpha_k \gtrless \alpha\} \to 0$, and $f(\alpha) = 1$ for all α on the real line. As expected, the spectrum is highly degenerate.

As a conclusion to this section, we note that the spectrum of a multiplicative measure is very sensitive to the distribution of its multiplier M. This property, sometimes called "gross non-universality", suggests that the MMAR has enough flexibility to model a wide range of financial prices.

5 Application to the Multifractal Model of Asset Returns

Having developed a theory for the local behavior of multifractal processes, we now examine the multifractal spectra of processes generated by the MMAR, which is now briefly recalled.

A financial time series is modeled as a stochastic process $\{P(t); 0 \le t \le T\}$. The transformed process:

$$X(t) = \ln P(t) - \ln P(0),$$

is viewed as a multifractal compound process that satisfies the following properties.

Assumption 1. *$X(t)$ is a compound process:*

$$X(t) \equiv B_H[\theta(t)]$$

where $B_H(t)$ is a fractional Brownian Motion with self-affinity index H, and $\theta(t)$ is a stochastic trading time.

Assumption 2. *The trading time $\theta(t)$ is the c.d.f. of a multifractal measure defined on $[0,T]$. That is, $\theta(t)$ is a multifractal process with continuous, non-decreasing paths, and stationary increments.*

Assumption 3. *$\{B_H(t)\}$ and $\{\theta(t)\}$ are independent.*

While Mandelbrot, Fisher and Calvet (1997) studied the scaling properties of the MMAR in terms of moments, this paper focuses on the local scaling properties of the price process. We denote $f_\theta(\alpha)$ the multifractal spectrum of the process trading time and establish the following theorem.

Theorem 7 *Under Assumptions $[1]-[3]$, the processes $X(t)$ and $P(t)$ have multifractal spectrum $f(\alpha) = f_\theta(\alpha/H)$.*

Proof. The infinitesimal variation of the transformed process $X(t)$ around date t satisfies:

$$\begin{aligned} |X(t+\triangle t) - X(t)| &= |B_H[\theta(t+\triangle t)] - B_H[\theta(t)]| \\ &\sim |\theta(t+\triangle t) - \theta(t)|^H \\ &\sim |\triangle t|^{H\alpha_\theta(t)}, \end{aligned}$$

where $\alpha_\theta(t)$ denotes the Hölder exponent of θ at t. The Hölder exponent of X at t is therefore equal to $H\alpha_\theta(t)$. The set of points where X has Hölder exponent α is then identical to the set of points where θ has Hölder exponent α/H. Therefore they have the same fractal dimension, and $f(\alpha) = f_\theta(\alpha/H)$.

Since $P(t)$ is a continuously differentiable function of $X(t)$, these two processes have the same local Hölder exponent and therefore the same spectra. ■

Theorem 5.1 shows that the MMAR contains a continuum of local Hölder exponents. Multifractality of the compound price process is entirely caused by the trading time, and accounts for scale consistency and persistence.

Long memory has an interesting geometric interpretation in this model. When the price process is multiscaling, several sets[6] $T(\alpha)$ have a non-integer fractal dimension $f(\alpha)$: $0 < f(\alpha) < 1$. Their elements necessarily cluster in certain regions of the interval of definition $[0, T]$, which explains the alternance of periods of large and small price changes. The set $T(\alpha)$ is also statistically self-similar in the sense that after proper rescaling, subsets of $T(\alpha)$ have statistically the same spreading of points than the original $T(\alpha)$. Therefore knowledge of $T(\alpha)$ in one period of time contains important information on $T(\alpha)$ in later periods. This property accounts for long memory in the process.

6 Conclusion

This paper examines the *local* scaling properties of multifractals. Our analysis builds on the concept of the local Hölder exponent, a positive real number that quantifies a function's singularity at a given date. In the spirit of fractal geometry, these exponents are interpreted as local scaling factors that can vary with time. Multifractals are then viewed as generalized fractal objects containing a *continuum* of scales.

The distribution of local Hölder exponents over time is described by the multifractal spectrum $f(\alpha)$, a renormalized density obtained as the limit of histograms. In an alternative interpretation, $f(\alpha)$ is viewed as the fractal dimension of the set of instants $T(\alpha)$ with local Hölder exponent α. The statistical self-similarity of the sets $T(\alpha)$ is closely related to the long memory. For a large class of multifractals, the spectrum can be explicitly derived from Cramér's Large Deviation Theory. We apply this idea on a number of examples, and note the sensitivity of the multifractal spectrum to the generating mechanism. This allows the applied researcher to relate an empirical estimate of the spectrum back to a particular construction of the multifractal.

Finally, we apply these ideas to the Multifractal Model of Asset Returns (MMAR). The heterogeneity of local scales along the price process is entirely attributable to the trading time $\theta(t)$. Moreover, the multifractal spectrum of the price process is derived from the spectrum of $\theta(t)$ by a very simple transformation. The multiscaling properties of the MMAR sharply contrast with

[6] As in Section 3.3, we denote $T(\alpha)$ the set of instants with Hölder exponent α.

the unique scale contained in previous financial models, including continuous Itô processes and fractional Brownian motions. They account for the main features of the MMAR: scale-consistency, fat tails, temporal heterogeneity and long memory in the magnitude of price changes. The results of this paper also suggest several directions for empirical research, such as estimating the multifractal spectrum and inferring the generating mechanism of a given price process. The companion empirical paper, Fisher, Calvet and Mandelbrot (1997), proposes some solutions to these problems. The development of estimation and inference methods for the MMAR should however be the focus of further research.

7 Appendix

7.1 The Hausdorff-Besicovitch Dimension

We consider a bounded subset A of the Euclidean space $\mathbb{R}^n$, $(n \geq 1)$. An open and countable covering of A consists of a family of open subsets $(U_i)_{i=1}^{\infty}$ that satisfies $A \subseteq \cup_{i=1}^{\infty} U_i$. For any positive real numbers s and ε, we define the quantity:

$$h_\varepsilon^s(A) = Inf \left\{ \sum_{i=1}^{\infty} diam(U_i)^s \mid (U_i)_{i=1}^{\infty} \text{ open covering of } A,\ diam(U_i) < \varepsilon \ for \text{ all i} \right\}.$$

As we decrease ε, the class of permissible coverings decreases, and the infimum increases. It thus converges to a limit:

$$h^s(A) = \lim_{\varepsilon \to 0} h_\varepsilon^s(A),$$

which belongs to $[0, \infty]$. It is then possible to prove the following result.

Proposition 8 *There exists a non-negative real number $D(A)$ such that $h^s(A) = \infty$ if $s < D(A)$ and $h^s(A) = 0$ if $s > D(A)$. We call $D(A)$ the fractal or Hausdorff-Besicovitch dimension of A.*

The fractal dimension satisfies the following properties:

- If $A \subseteq \mathbb{R}^n$, then $D(A) \leq n$.
- If $A \subseteq B$, then $D(A) \leq D(B)$.
- If A is a countable set, then $D(A) = 0$.

7.2 Proof of Proposition 4.2

We easily see that:

$$\begin{aligned}
\mathbb{P}\left\{\overline{\alpha}_j < \alpha_k \leq \overline{\alpha}_j + \Delta\alpha\right\} &= \mathbb{P}\left\{\alpha_k > \overline{\alpha}_j\right\} - \mathbb{P}\left\{\alpha_k > \overline{\alpha}_j + \Delta\alpha\right\} \\
&= \mathbb{P}\{\alpha_k > \overline{\alpha}_j\} \left[1 - \frac{\mathbb{P}\{\alpha_k > \overline{\alpha}_j + \Delta\alpha\}}{\mathbb{P}\{\alpha_k > \overline{\alpha}_j\}}\right] \\
&\sim \mathbb{P}\{\alpha_k > \overline{\alpha}_j\}
\end{aligned}$$

The last equality follows from the fact that $\delta(\overline{\alpha}_j + \Delta\alpha) < \delta(\overline{\alpha}_j)$, and thus that the ratio

$$\frac{\mathbb{P}\{\alpha_k > \overline{\alpha}_j + \Delta\alpha\}}{\mathbb{P}\{\alpha_k > \overline{\alpha}_j\}} \sim (b^k)^{\delta(\overline{\alpha}_j + \Delta\alpha) - \delta(\overline{\alpha}_j)}$$

vanishes as $k \to \infty$.

7.3 Binomial Distribution

It is straightforward to compute $f(\alpha)$ by a Legendre transform of $\tau(q)$, which establishes (13) under definition $(D3)$.

The same result also holds under definition $(D1)$. With the notations of Section 3.2, we consider a fixed interval $(\overline{\alpha}_j, \overline{\alpha}_j + \Delta\alpha]$ and seek to compute the limit of $\log_2 N_k(\overline{\alpha}_j)/k$. The indices are chosen so that $\alpha_{\max} = -\log_2 m_{0.}$ After k iterations, the coarse Hölder exponent of a b-adic interval is of the form:

$$\alpha_k(t) = (\alpha_{\max} - \alpha_{\min})\varphi_{0,k}(t) + \alpha_{\min},$$

where $\varphi_{0,k}(t)$ is the relative frequency of m_0's drawn in the construction. We observe that there is a one-to-one correspondence between $\alpha_k(t)$ and $\varphi_{0,k}(t)$. For this reason, it is convenient to define

$$\overline{\varphi}_j = \frac{\overline{\alpha}_j - \alpha_{\min}}{\alpha_{\max} - \alpha_{\min}} \tag{14}$$

and $\Delta\varphi = \Delta\alpha/(\alpha_{\max} - \alpha_{\min})$. The integer $N_k(\overline{\alpha}_j)$ can now be rewritten:

$$\begin{aligned} N_k(\overline{\alpha}_j) &= Card\left\{t_i \text{ s.t. } \varphi_{0,k}(t_i) \in (\overline{\varphi}_j, \overline{\varphi}_j + \Delta\varphi]\right\} \\ &= \sum_{l=[k\overline{\varphi}_j]+1}^{[k(\overline{\varphi}_j+\Delta\varphi)]} \begin{pmatrix} k \\ l \end{pmatrix}, \end{aligned}$$

the last formula being obtained by a simple combinatorial argument.

We first consider the case $\overline{\alpha}_j > \alpha_0$, i.e. $\overline{\varphi}_j > 1/2$. The inequalities

$$\begin{pmatrix} k \\ [k\overline{\varphi}_j]+1 \end{pmatrix} \leq N_k(\overline{\alpha}_j) \leq \left([k(\overline{\varphi}_j + \Delta\varphi)] - [k\overline{\varphi}_j]\right) \begin{pmatrix} k \\ [k\overline{\varphi}_j]+1 \end{pmatrix},$$

imply the useful equivalence

$$\frac{1}{k}\log_2 N_k(\overline{\alpha}_j) \sim \frac{1}{k}\log_2 \begin{pmatrix} k \\ [k\overline{\varphi}_j]+1 \end{pmatrix} \qquad \text{as } k \to \infty.$$

Stirling 's approximation can be applied to the right-hand side:

$$\frac{1}{k}\log_2 N_k(\overline{\alpha}_j) \to -\overline{\varphi}_j \log_2 \overline{\varphi}_j - (1 - \overline{\varphi}_j)\log_2(1 - \overline{\varphi}_j).$$

Using (14), we substitute $\overline{\varphi}_j$ in this equation and obtain (13). A similar reasoning holds for $\overline{\alpha}_j < \alpha_0$.

7.4 Poisson Distribution

We choose a real number $\alpha > \alpha_0 = \gamma$. Since

$$\mathbb{P}\{\alpha_k > \alpha\} = \mathbb{P}\{V_1 + .. + V_k > k\alpha\} = \sum_{x=[k\alpha]+1}^{\infty} e^{-k\gamma} \frac{(k\gamma)^x}{x!},$$

we know that:

$$\begin{aligned} \frac{1}{k} \log_b \mathbb{P}\{\alpha_k &> \alpha\} = \frac{1}{k} \log_b \left[e^{-k\gamma} \frac{(k\gamma)^{[k\alpha]+1}}{([k\alpha]+1)!} \sum_{x=0}^{\infty} (k\gamma)^x \frac{([k\alpha]+1)!}{(x+[k\alpha]+1)!} \right] \\ &= \frac{1}{k} \log_b \left[e^{-k\gamma} \frac{(k\gamma)^{[k\alpha]+1}}{([k\alpha]+1)!} \right] + \frac{1}{k} \log_b \left[\sum_{x=0}^{\infty} (k\gamma)^x \frac{([k\alpha]+1)!}{(x+[k\alpha]+1)!} \right]. \end{aligned}$$

The limit behavior of the two addends is successively examined. First Sterling's approximation implies that:

$$\frac{1}{k} \log_b \left[e^{-k\gamma} \frac{(k\gamma)^{[k\alpha]+1}}{([k\alpha]+1)!} \right] \to -\frac{\gamma}{\ln b} + \alpha \log_b(\gamma e/\alpha).$$

Second, since

$$(k\gamma)^x \frac{([k\alpha]+1)!}{(x+[k\alpha]+1)!} \leq \frac{(k\gamma)^x}{([k\alpha]+2)^x} \leq \left(\frac{\gamma}{\alpha}\right)^x,$$

the expression $\sum_{x=0}^{\infty} (k\gamma)^x ([k\alpha]+1)!/(x+[k\alpha]+1)!$ is bounded, and thus

$$\frac{1}{k} \log_b \left[\sum_{x=0}^{\infty} (k\gamma)^x \frac{([k\alpha]+1)!}{(x+[k\alpha]+1)!} \right] \to 0.$$

A similar reasoning holds for $\alpha < \gamma$.

References

[1] Billingsley (1967), *Ergodic Theory and Information*, New York: Wiley

[2] Deutschel, J. D., and Stroock, D. W. (1989), *Large Deviations*, New York: Academic Press

[3] Durrett, R. (1991), *Probability: Theory and Examples*, Pacific Grove, Calif.: Wadsworth & Brooks/Cole Advanced Books & Software

[4] Evertsz, C. J. G., and Mandelbrot, B. B. (1992), Multifractal Measures, in: Peitgen, H. O., Jürgens, H., and Saupe, D. (1992), *Chaos and Fractals: New Frontiers of Science*, 921-953, New York: Springer Verlag

[5] Fisher, A., Calvet, L., and Mandelbrot, B. B. (1997), Multifractality of Deutschmark/US Dollar Exchange Rates, Yale University, Working Paper

[6] Frisch, U., and Parisi, G. (1985), Fully Developed Turbulence and Intermittency, in: M. Ghil ed., *Turbulence and Predictability in Geophysical Fluid Dynamics and Climate Dynamics*, 84-88, Amsterdam: North-Holland

[7] Halsey, T. C., Jensen, M. H., Kadanoff, L. P., Procaccia, I., and Shraiman, B. I. (1986), Fractal Measures and their Singularities: The Characterization of Strange Sets, *Physical Review Letters A* **33**, 1141

[8] Hausdorff, F. (1919), Dimension und äusseres Mass, *Mathematische Annalen* **79** 157-179

[9] Mandelbrot, B. B., and Ness, J. W. van (1968), Fractional Brownian Motion, Fractional Noises and Application, *SIAM Review* **10**, 422-437

[10] Mandelbrot, B. B. (1982), *The Fractal Geometry of Nature*, New York: Freeman

[11] Mandelbrot, B. B. (1989a), Multifractal Measures, Especially for the Geophysicist, *Pure and Applied Geophysics* **131**, 5-42

[12] Mandelbrot, B. B. (1989b), Examples of Multinomial Multifractal Measures that Have Negative Latent Values for the Dimension $f(\alpha)$, in: L. Pietronero ed., *Fractals'Physical Origins and Properties,* 3-29, New York: Plenum

[13] Mandelbrot, B. B. (1990), Limit Lognormal Multifractal Measures, in: E. A. Gotsman et al. eds., *Frontiers of Physics: Landau Memorial Conference*, 309-340, New York: Pergamon

[14] Mandelbrot, B. B., Fisher, A., and Calvet, L. (1997), The Multifractal Model of Asset Returns, Yale University, Working Paper

[15] Peyrière, J. (1991), Multifractal Measures, in *Proceedings of the NATO ASI "Probabilistic Stochastic Methods in Analysis, with Applications"*

[16] Rogers, C. A. (1970), *Hausdorff Measures*, Cambridge University Press

[17] Rossi, P. ed. (1997), *Modeling Stock Market Volatility: Bridging the Gap to Continuous Time*, New York: Academic Press

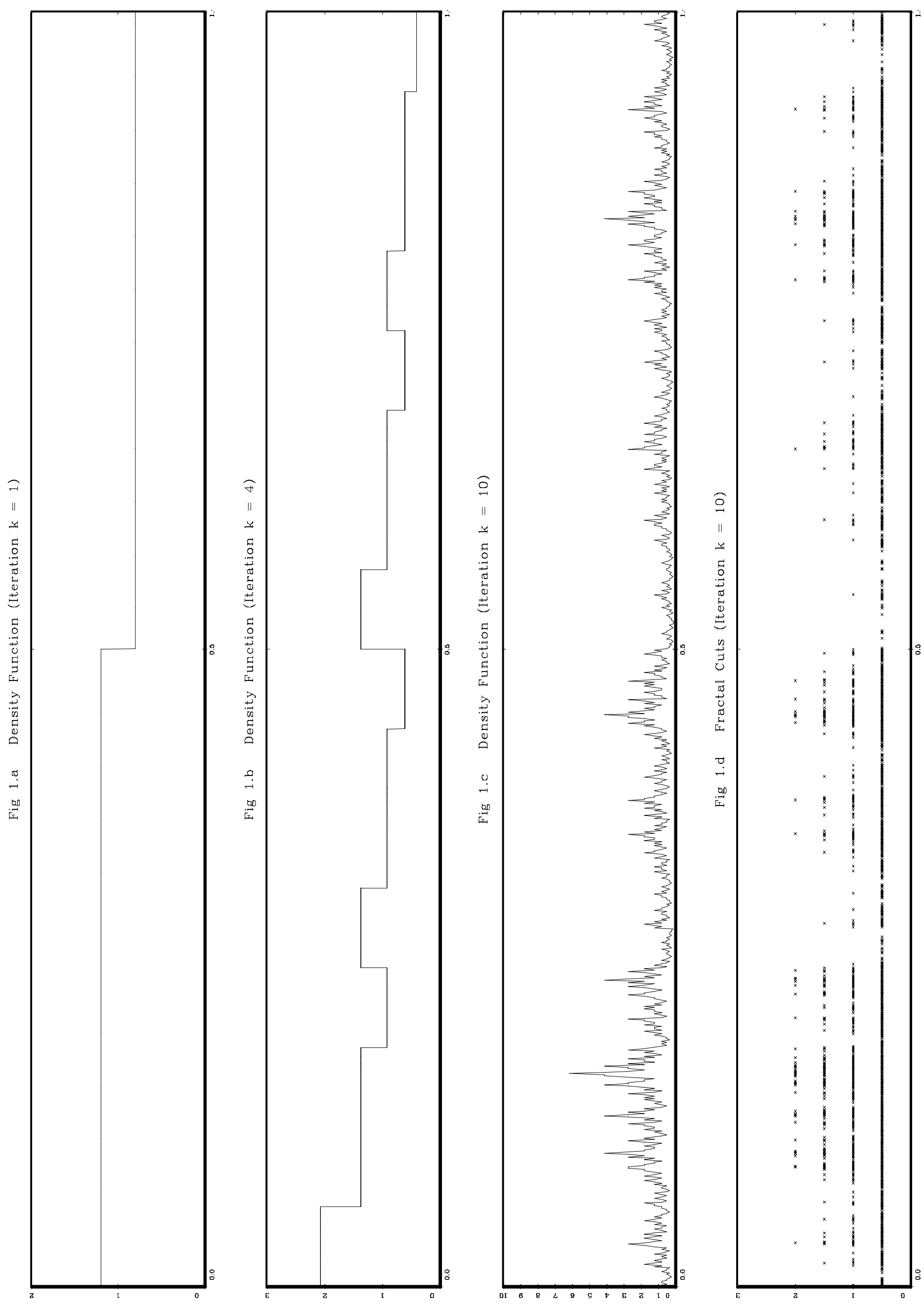

Fig 1.a Density Function (Iteration k = 1)

Fig 1.b Density Function (Iteration k = 4)

Fig 1.c Density Function (Iteration k = 10)

Fig 1.d Fractal Cuts (Iteration k = 10)

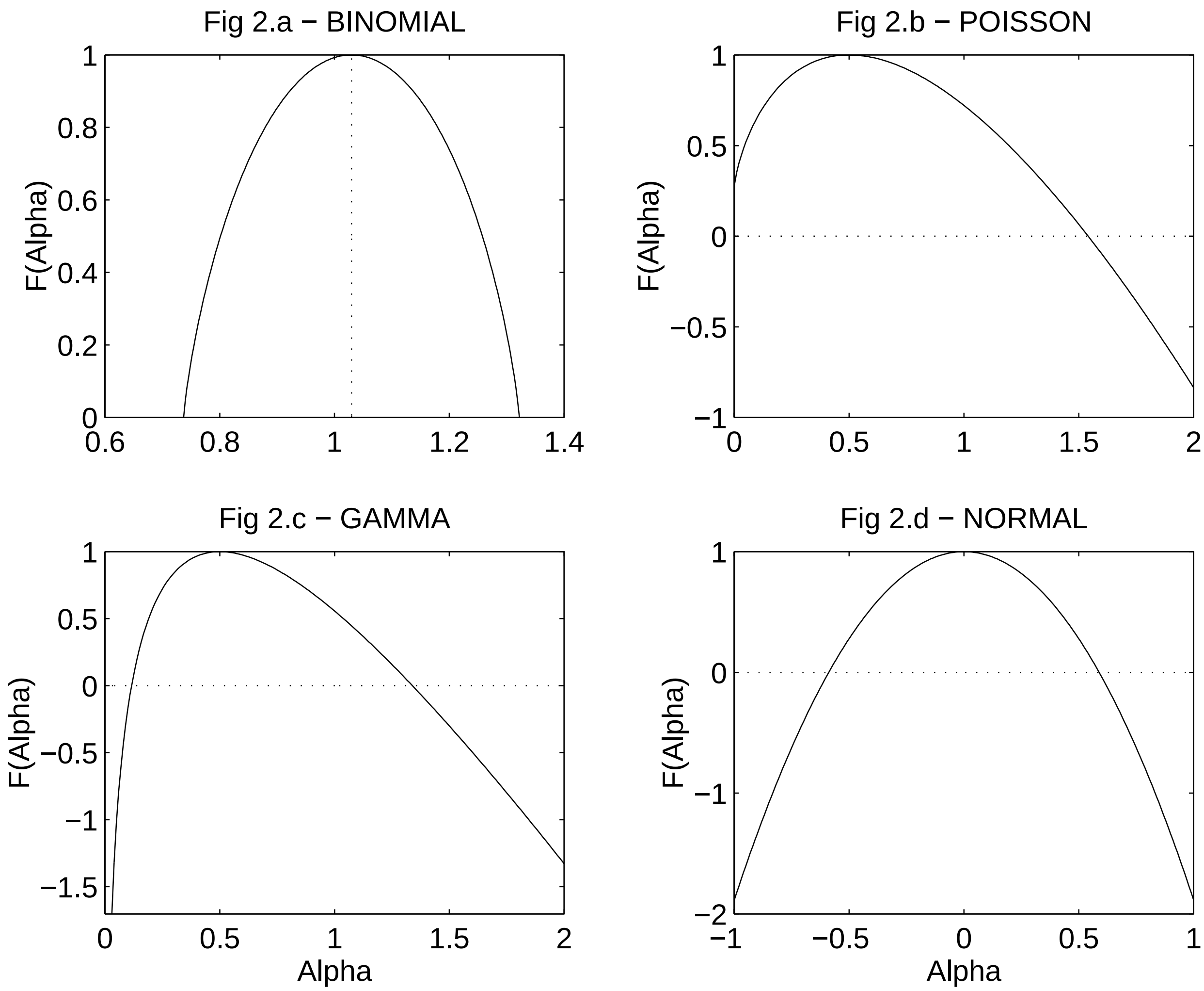
Fig 2.a − BINOMIAL
Fig 2.b − POISSON
Fig 2.c − GAMMA
Fig 2.d − NORMAL
F(Alpha)
Alpha